De Novo Variants in *WDR37* Are Associated with Epilepsy, Colobomas, Dysmorphism, Developmental Delay, Intellectual Disability, and Cerebellar Hypoplasia

Oguz Kanca,[1] Jonathan C. Andrews,[1] Pei-Tseng Lee,[1] Chirag Patel,[2] Stephen R. Braddock,[3,4] Anne M. Slavotinek,[5] Julie S. Cohen,[6] Cynthia S. Gubbels,[7] Kimberly A. Aldinger,[8] Judy Williams,[9] Maanasa Indaram,[10] Ali Fatemi,[6] Timothy W. Yu,[7] Pankaj B. Agrawal,[11] Gilbert Vezina,[12] Cas Simons,[13,14] Joanna Crawford,[13] C. Christopher Lau,[15] Undiagnosed Diseases Network,[16] Wendy K. Chung,[17] Thomas C. Markello,[15,18] William B. Dobyns,[8,19,20] David R. Adams,[15,18] William A. Gahl,[15,18] Michael F. Wangler,[1,21,22] Shinya Yamamoto,[1,21,22,23] Hugo J. Bellen,[1,21,22,23,24,*] and May Christine V. Malicdan[15,18,*]

WD40 repeat-containing proteins form a large family of proteins present in all eukaryotes. Here, we identified five pediatric probands with *de novo* variants in *WDR37,* which encodes a member of the WD40 repeat protein family. Two probands shared one variant and the others have variants in nearby amino acids outside the WD40 repeats. The probands exhibited shared phenotypes of epilepsy, colobomas, facial dysmorphology reminiscent of CHARGE syndrome, developmental delay and intellectual disability, and cerebellar hypoplasia. The WDR37 protein is highly conserved in vertebrate and invertebrate model organisms and is currently not associated with a human disease. We generated a null allele of the single *Drosophila* ortholog to gain functional insights and replaced the coding region of the fly gene *CG12333/wdr37* with GAL4. These flies are homozygous viable but display severe bang sensitivity, a phenotype associated with seizures in flies. Additionally, the mutant flies fall when climbing the walls of the vials, suggesting a defect in grip strength, and repeat the cycle of climbing and falling. Similar to wall clinging defect, mutant males often lose grip of the female abdomen during copulation. These phenotypes are rescued by using the GAL4 in the *CG12333/wdr37* locus to drive the UAS-human reference *WDR37* cDNA. The two variants found in three human subjects failed to rescue these phenotypes, suggesting that these alleles severely affect the function of this protein. Taken together, our data suggest that variants in *WDR37* underlie a novel syndromic neurological disorder.

WD40 repeats (WDRs) are among the most abundant protein-protein interaction domains in eukaryotic proteins. WDRs are stretches of ~40 amino acid repeats that often terminate in tryptophan (W) and aspartic acid (D) residues and constitute the fourth most abundant protein domain in the human genome. In yeast, WDRs participate in more protein-protein interactions than any other protein domains.[1] The HUGO Gene Nomenclature Committee (HGNC)[2] annotates 274 genes that encode WDR-containing proteins including 60 that are already associated with diseases in OMIM. WDR proteins have been implicated in a wide range of functions and in a variety of diseases (Table S1).

Here, we report the identification of five individuals with missense *de novo* variants in *WDR37* who have several shared phenotypes including ocular colobomas, cerebellar malformations, developmental delay and intellectual disability, facial dysmorphism, and epilepsy. The first proband was identified through the Undiagnosed Diseases Network,[3–5] and subsequent searches of collaborative genomic databases, including GeneMatcher[6] and MyGene2[7] led to the identification of four additional individuals reported here. All probands were evaluated under clinical protocols approved by the respective institutional review boards (IRB) in the institutions/hospitals where they were evaluated: proband 1, NIH-UDP 76-HG-0238 and 15-HG-0130 protocols approved by the National Human Genome Research Institute (NHGRI) IRB; proband 2, "Use of High Throughput Genomic Sequencing

[1]Department of Molecular and Human Genetics, Baylor College of Medicine, Houston, TX 77030, USA; [2]Genetic Health Queensland, Royal Brisbane and Women's Hospital, Brisbane, QLD 4029, Australia; [3]Division of Medical Genetics, SSM Health Cardinal Glennon Children's Medical Center, St. Louis, MO 63104, USA; [4]Department of Pediatrics, Saint Louis University Hospital, St. Louis, MO 63104, USA; [5]Department of Pediatrics, University of California, San Francisco, CA 94143-2711, USA; [6]Division of Neurogenetics and Hugo W. Moser Research Institute, Kennedy Krieger Institute, Baltimore, MD 21205, USA; [7]Division of Genetics and Genomics, Boston Children's Hospital/Harvard Medical School/Broad Institute of MIT and Harvard, Boston, MA 02138, USA; [8]Center for Integrative Brain Research, Seattle Children's Research Institute, Seattle, WA 98101, USA; [9]Paediatric Department, Bundaberg Hospital, Bundaberg, QLD 4670, Australia; [10]Department of Ophthalmology, University of California, San Francisco, CA 94143-2711, USA; [11]Division of Newborn Medicine and Genetics and Genomics, Manton Center for Orphan Disease Research, Harvard Medical School, Boston, MA 02115, USA; [12]Division of Diagnostic Imaging & Radiology, Children's National Health System, 111 Michigan Ave. NW, Washington, DC 20010, USA; [13]The Institute of Molecular Bioscience, The University of Queensland, Brisbane, QLD 4072, Australia; [14]Murdoch Childrens Research Institute, Melbourne, VIC 3052 Australia; [15]NIH Undiagnosed Diseases Program, Common Fund, Office of the Director, NIH, Bethesda, MD 20892, USA; [16]Undiagnosed Diseases Network, Common Fund, Office of the Director, National Institutes of Health, Bethesda, MD 20892, USA; [17]Department of Pediatrics and Medicine, Columbia University, New York, NY 10032, USA; [18]Office of the Clinical Director, National Human Genome Research Institute, NIH, Bethesda, MD 20892-1851, USA; [19]Department of Pediatrics (Genetics), University of Washington, Seattle, WA 98195, USA; [20]Department of Neurology, University of Washington, Seattle, WA 98195, USA; [21]Program in Developmental Biology, Baylor College of Medicine, Houston, TX 77030, USA; [22]Jan and Dan Duncan Neurological Research Institute, Texas Children's Hospital, Houston, TX 77030, USA; [23]Department of Neuroscience, Baylor College of Medicine, Houston, TX 77030, USA; [24]Howard Hughes Medical Institute, Baylor College of Medicine, Houston, TX 77030, USA
*Correspondence: hbellen@bcm.edu (H.J.B.), maychristine.malicdan@nih.gov (M.C.V.M.)
https://doi.org/10.1016/j.ajhg.2019.06.014.

Figure 1. Clinical Features of Probands
All probands exhibit facial dysmorphisms.
(A and B) Proband 1 (P1) has a tall forehead, broad nasal bridge, flat philtrum with a thin vermillion border, low-set ears, and small jaw.
(C and D) Proband 2 (P2) has hypertelorism, ptosis, long eyelashes, left iris coloboma, prominent nasal bridge, short smooth philtrum, thin upper lip, downturned corners of the mouth, and low-set ears with thick prominent helices.
(E) Proband 3 (P3) has excess nuchal skin, visible epicanthal folds, broad nasal bridge, and smooth philtrum.
(F and G) Proband 4 (P4) has epicanthal folds, ectropion of lower lids, wide mouth with downturned corners, smooth philtrum, and prominent nose.

Technologies for Gene Discovery in Genetic diseases" approved by the IRB of The Royal Brisbane and Women's Hospital; probands 3 and 4, IRB-AAAJ8651, approved by the IRB of Columbia University; and proband 5, "The Manton Center for Orphan Disease Research Gene Discovery Core (GDC), approved by the IRB of Boston Children's Hospital. Permission to include the photographs were obtained from the parents of the probands.

Proband 1, a 7-year-old boy, was born with a short umbilical cord, intestinal malrotation repaired at 2 days of life, hypotonia, severe feeding abnormalities, and neonatal-onset seizures. He had global developmental delay and by age 7 years was unable to walk or use any words or signs, consistent with severe intellectual disability. Dysmorphic facial features included a tall forehead, broad nasal bridge, flat philtrum with a thin vermillion border, low-set ears, and small jaw (Figure 1). He had Peters' anomaly on the left eye (corneal clouding with central corneal leukoma, multiple iris adhesions, microcornea, and congenital glaucoma), iris coloboma and mild microcornea without Peters' anomaly on the right, and bilateral chorioretinal colobomas, more severe on the left. Other anomalies included bilateral moderate sensorineural hearing loss, persistent patent foramen ovale, possible small ventriculoseptal defect, hand and foot syndactyly, right hydronephrosis, micropenis with chordee and possible hypospadias, and undescended testes. A brain MRI at 11 months demonstrated decreased cerebral volume with severely reduced white matter volume, thin corpus callosum, moderate cerebellar vermian hypoplasia, mild cerebellar hemisphere hypoplasia, enlarged posterior fossa size, and other abnormalities (Figure 2). Images through the eyes showed thin optic nerves and a small coloboma in the posterior left eye.

Proband 2, a 6-year-old girl, was born at 38 4/7 weeks of gestation with respiratory distress and hypotonia. She failed to thrive and developed postnatal microcephaly. Generalized tonic clonic seizures on day 5 required anticonvulsants until 8 months of age but she has been seizure-free since then. She had ventricular and atrial septal defects, patent ductus arteriosus and tricuspid regurgitation, with corrective surgery at 8 months. Brain MRI scan showed cerebellar vermian hypoplasia and dysplasia, mild pons hypoplasia, gray matter heterotopias within the right frontal lobe, and a pericallosal lipoma (Figure 2). She has bilateral colobomas and small optic nerves, and wears glasses. She has bilateral low-tone sensorineural hearing loss, significant developmental delay, and intellectual impairment. Physical findings include hypertelorism (+2 SD), ptosis, long eyelashes, left iris coloboma, prominent nasal bridge, short smooth philtrum, thin upper lip, downturned corners of the mouth, low-set ears with thick prominent helices (Figure 1), bilateral single palmar creases, joint laxity, and bilateral talipes.

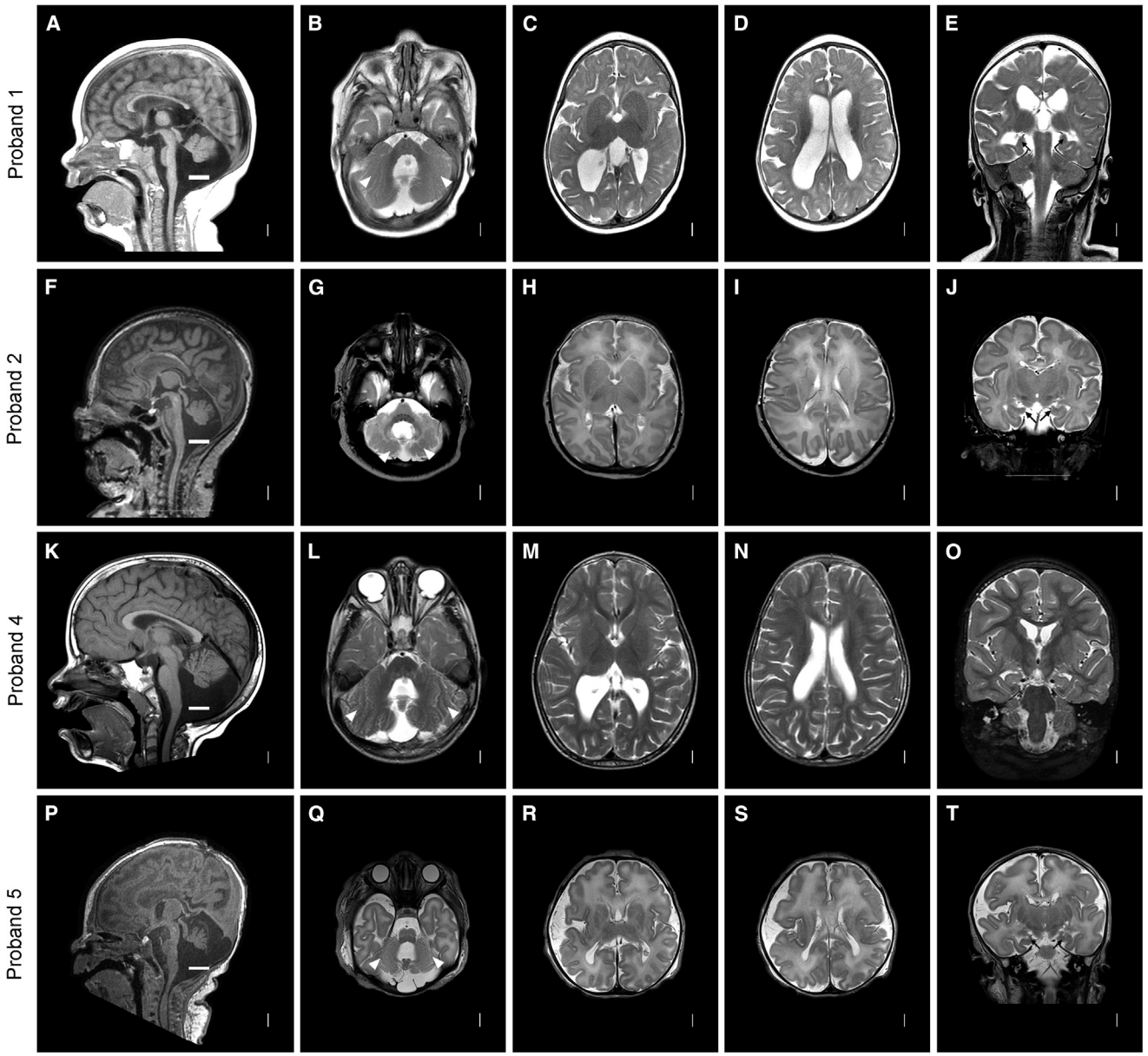

Figure 2. Brain MRI Images in Probands 1, 2, 4, and 5
Shown are probands 1 (A–E), 2 (F–J), 4 (K–O), and 5 (P–T). Midline sagittal images show mild (K) or severe (A, F, P) cerebellar vermis hypoplasia; the horizontal white bars mark the expected lower edge of the vermis near the obex. Axial T2-weighted images through the posterior fossa (B, G, L, Q) show enlarged 4th ventricle and small cerebellar hemispheres with a striking foliar dysplasia (white arrowheads). Axial T2-weighted images through the cerebral hemispheres (third and fourth columns) show diffuse shallow sulci or simplified gyral pattern, reduced white matter volume, and mild ventriculomegaly. Coronal T2-weighted images show striking hippocampal hypoplasia and dysplasia in 3 of 5 subjects (black arrows in E, J, T). Note: for proband 3, only limited MRI images were available for review. For comparison, please refer to the studies of Sanchez et al.[32] for MRI images in control individuals.

Proband 3, an 8-month-old girl, has bilateral iris colobomas, excess nuchal skin, wide-spaced and inverted nipples, abnormal ear shape (mildly dysplastic helices), visible epicanthal folds, broad nasal bridge, a broad hallux, and minimally overlapping toes. Her hospitalization was complicated by seizures, which were controlled with fosphenytoin and carbamazepine, direct hyperbilirubinemia, pulmonary hypertension, pulmonary edema, patent ductus arteriosus that was surgically corrected, and a muscular ventriculoseptal defect. Brain MRI at day 12 showed dilatation of the fourth ventricle and hypoplasia of the cerebellar vermis and mildly diminished white matter parenchymal volume (Figure S1). There were bilateral iris, chorioretinal, and optic nerve colobomas, with the left optic nerve more severely affected than the right.

Proband 4, a 19-year-old white female, had bilateral iris plus retinal-optic nerve colobomas at birth, as well as hydronephrosis and dilatation of the ureters, and left duplicated collecting system. She was hypotonic and developmentally delayed, but gradually became spastic.

She has severe intellectual disability and depends on others for all activities of daily living. She has short stature, colobomas, visible epicanthal folds, ectropion of lower lids, wide mouth with downturned corners, prominent nose (Figure 1), abnormal palmar creases, and bilateral short fifth fingers with clinodactyly. Generalized seizures were well controlled by topiramate. Brain MRI at 7 years showed moderate hypoplasia of the cerebellar vermis, disorganized cerebellar hemispheric folia, colpocephaly with a thin and elongated posterior corpus callosum, and bilateral colobomas (Figure 2).

Proband 5, a male infant, had two-vessel umbilical cord, micropenis, cryptorchidism, eye abnormalities (cloudy cornea, microcornea, microphthalmia), dysmorphic features, and a cardiac murmur at birth. He developed seizures on day 2, with apneas requiring intubation and oxygenation on day 6. He had bilateral microphthalmia, microcornea, bilateral congenital aphakia, and bilateral congenital glaucoma, with elevated intraocular pressure in both eyes, reflecting anterior segment dysgenesis. Brain MRI on day 4 showed moderate vermian hypoplasia (Figure 2), ventral pontine hypoplasia, disorganized cerebellar foliar pattern, bilateral perisylvian polymicrogyria, corpus callosal dysgenesis, large massa intermedia, optic nerve hypoplasia, small globes, and aphakia. Echocardiogram on day 5 revealed a large secundum atrial septal defect with left-to-right flow, several tiny muscular ventricular septal defects, right ventricle dilation and hypertrophy, mild right ventricular dysfunction, and low normal left ventricular systolic function. Nasogastric tube feeding was required up to age 4 weeks.

A summary of the clinical features and molecular findings of the five probands are in Tables 1, 2, and S2. Additional clinical data are found in Supplemental Note: Case Reports. All of the probands had eye anomalies (bilateral colobomas in 4 of 5 probands; microphthalmia in 3 of 5); dysmorphic features (most had prominent forehead, wide, downturned mouth, excessive nuchal skin, and broad nasal bridge; 3/5 had wide-spaced nipples); seizures; and feeding difficulties. Developmental delay, intellectual disability, and no verbal development was in 4 probands, although proband 5 is too young for evaluation. Follow-up studies to determine whether proband 5 will develop intellectual disability will further delineate the clinical spectrum of this disorder. Most of the probands had congenital cardiac defects (4 of 5), hypotonia (4 of 5), postnatal microcephaly (3 of 5), and hearing loss (2 of 5; no hearing test was performed in proband 5). The two male probands included in the study both had micropenis and undescended testes.

The brain malformations proved to be remarkably similar among all five probands. The key features included (1) diffuse gyral hypoplasia due to thin or narrow gyri with reduced white matter, (2) mildly small and dysplastic hippocampi, (3) diffusely reduced volume of white matter, (4) mildly enlarged lateral ventricles, (5) diffusely thin corpus callosum with callosal lipoma in 1 of 5 subjects (6) unusually thin anterior commissure (7) mild diffuse brainstem hypoplasia that was most obvious in the pons, (8) diffuse mild or moderate cerebellar hypoplasia with diffuse and strikingly abnormal foliar pattern, (9) sometimes mildly enlarged size of the posterior fossa, (10) posterior eye (retinal) colobomas, and (11) optic nerve hypoplasia. No specific cortical malformations were seen. In proband 2, there was mild subcortical heterotopia in the right mid-frontal lobe and a lipoma in the corpus callosum in proband 2 (LR17-513).

Whole-exome sequencing was performed on four probands at three different research centers to identify pathogenic variants underlying their disease (see Supplemental Note: Case Reports and Figure S1); whole-genome sequencing was performed on proband 2. Variant interpretation and prioritization were based on the clinical relevance of the gene and the pathogenicity of the variants using the ACMG-AMP guidelines,[8] Mendelian consistency and segregation, observed frequency of the variants in public and internal population databases, conservation, and predicted deleteriousness of the candidate genes (for further details, see Supplemental Note: Case Reports).

All the probands shared *de novo* missense variants in *WDR37* (Table 3). To perform a comprehensive database search on *WDR37*, we utilized MARRVEL (Model organism Aggregated Resources for Rare Variant ExpLoration), which aggregates data from multiple databases including ExAC, gnomAD, and OMIM among others.[9] The variants in our cohort were not observed ExAC and gnomAD and were predicted to be pathogenic by PROVEAN and PolyPhen2 (see Web Resources). The *WDR37* gene contains an identifiable coiled coil region and seven WDRs (Figure 3A). WDRs are suggested to form 8 bladed beta propeller folds that form protein interaction interfaces.[1] These repeats are found in a variety of proteins and do not confer sufficient information *per se* to suggest functionality. Despite a lack of functional data, human population genetic data suggest that *WDR37* is somewhat intolerant of loss-of-function (LoF) variations, with a pLI (probability of LoF intolerance) score of 0.57 based on gnomAD with e/o (expected/observed) ratio of 0.21.[10] There are two early frameshift variants in gnomAD (p.Phe62Valfs*3 and p.Arg67Asnfs*10) likely resulting in LoF in control individuals. In addition, there are 25 copy number variants in DECIPHER database with diverse phenotypes but the large size of deleted regions limit the specificity of the phenotypes.[11] Additionally there is one deletion identified in 1000 Genomes project from a healthy individual's immortalized blood cells.[12] Missense variants in *WDR37* are selected against in the general population because it exhibits missense constraint with a z score of 2.31 in gnomAD. All but one (p.Leu77Ile) missense variant found in these public databases (ExAC, gnomAD) are heterozygous. All the variants that we present in this cohort are absent in ExAC and gnomAD databases.[10]

The affected residues in the probands are located between the amino-terminal coiled coil region and the first

Table 1. Summary of Clinical Features of Probands with *De Novo WDR37* Variants

Clinical Feature	Proband 1	Proband 2	Proband 3	Proband 4	Proband 5	Summary
Abnormal cerebellum morphology (HP:0001317)	+	+	+	+	+	5/5
Epilepsy (HP:0001250)	+	+	+	+	+	5/5
Congenital heart defect (HP:0001627)	+, persistent foramen ovale, VSD	+, VSD, ASD, PDA, tricuspid regurgitation	+, VSD, PDA	–[a]	ASD, cardiomegaly	4/5
Coloboma (HP:0000589)	+, bilateral	+, bilateral	+, bilateral	+, bilateral	–	4/5
Developmental delay (HP:0001263)	+	+	+	+	undetermined	4/5
Intellectual disability (HP:0001249)	+	+	+	+	undetermined	4/5
Absent speech (HP:0001344)	+	+	+	+	undetermined	4/5
Postnatal microcephaly (HP:0005484)	+	+	–	+	NR	3/5
Microphthalmia (HP:0000568)	+, left	+, left	–	–	+, bilateral	3/5
Peters' anomaly (HP:0000659)	+, left	–	–	–	–	1/5
SNHL (HP:0000407)	+	+	–[b]	–	not done	2/5
Dysmorphic Features						
Downturned mouth (HP:0002714)	+	+	+	+	+	5/5
Prominent nasal bridge (HP:0000426)	+	+	+	+	+	5/5
Abnormality of the palmar creases (HP:0010490)	+, irregular and bridged	+, single palmar crease	+, hockey stick crease	+	+, diminished	5/5
Smooth philtrum (HP:000319)	+	+	+	+	undetermined	4/5
Prominent/tall forehead (HP:0011220)	+	+	+	+	–	4/5
Epicanthal folds (HP:0000286)	–	–	+	+	–	2/5
Hypertelorism (HP:0000316)	–	+	+	–	–	2/5
Low set ears (HP:0000369)	+	+	–	–	+	3/5
Wide-spaced nipples (HP:0006610)	+	–	+	–	+	3/5
Excessive nuchal skin (HP:0005989)	–	–	+	–	+	2/5
Micropenis (HP:0000054)	+	NA	NA	NA	+	2/2
Cryptorchidism (HP:0000028)	+	NA	NA	NA	+	2/2

Abbreviations: VSD, ventricular septal defect; ASD, atrial septal defect; PDA, patent ductus arteriosus; EEG, electroencephalogram; +, present; –, absent; NR, not reported; NA, not applicable; FO, foramen ovale; VSD, ventricular-septal defect; PDA, patent ductus arteriosus; ASD, atrial septal effect; TR, tricuspid regurgitation; SNHL, sensorineural hearing loss.
[a]Normal echocardiography as an infant, but more recently found with dilated aorta and aortic root
[b]Passed newborn exam

WD40 repeat. This domain (aa106–152) is also evolutionarily conserved from flies to vertebrates and is present only in WDR37 protein orthologs across species (Figure 3A). Despite the high level of conservation throughout the entire protein across species, there is remarkably little knowledge about the function of *WDR37* and its orthologs. The gene was targeted by the International Mouse Phenotyping Consortium (IMPC),[13] a large-scale mouse knock-out consortium, and routine phenotyping documented that the homozygous knockout animals are viable with mild neurological (decreased grip strength) and skeletal (kyphosis and fusion of vertebral arches) phenotypes. The hematologic findings include increased number of monocytes and $CD4^{+}CD25^{-}$ T cells and a decrease in B cells and total leukocytes. Biochemical findings include an increase in circulating calcium and alkaline phosphatase levels.[13]

To functionally annotate *WDR37* and to determine the functional consequences of the first two genetic variants that we identified, we studied the orthologous gene in *Drosophila melanogaster*.[14–16] *WDR37* has a single uncharacterized fly ortholog, *CG12333*, with high homology (DIOPT[17] score 14/15, 51% amino acid identity and 63% similarity) (Figure 3A). Due to high homology we named the gene *wdr37*.

Since there were no reported mutant alleles for *CG12333/wdr37*, we generated a null allele of *wdr37* by CRISPR-Cas9-directed homologous recombination[18–20] (Figure 3B, see Supplemental Material and Methods). We replaced the entire coding sequence of the gene with

Table 2. Brain Imaging Abnormalities in Children with *WDR37* Variants

	Subjects				
Proband Number	1	2	3	4	5
Code reference	LR13-199	LR17-513	LR18-508	LR18-509	LR18-510
Gyral hypoplasia	+	+	NA	+	+
Hippocampal dysplasia	+	+	NA	+	+
White matter hypoplasia	++	+	NA	+	+
Enlarged lateral ventricles	++	–	NA	+	+
Massa intermedia (thalami) large	++	+	+	+/–	++
Corpus callosum hypoplasia (thin)	++	+	+	+	++
Thin anterior commissure	–	+	NA	+	+
Brainstem hypoplasia (especially pons)	+	+	+	–	+
Cerebellar hypoplasia	++	++	++	+	++
Foliar dysgenesis, diffuse	++	++	NA	+	++
Posterior fossa, enlarged	+	–	–	+	+
Coloboma retina	L	L	L/R	L/R	–
Additional findings	optic nerve hypoplasia (thin)	corpus callosum lipoma; small subcortical heterotopia in right mid-frontal lobe			

Abbreviations: L, left; R, right; +, feature present; ++, feature present and moderate to severe; –, feature absent; NA, feature not available for review.

GAL4 in order to determine the expression pattern of the gene using UAS-GFP and to assess rescue of the induced mutation with a UAS-human *WDR37* cDNA to "humanize" the flies.[15,21] To create the GAL4 replacement, we injected two gRNAs that target the 5′ and 3′ UTR and a template carrying homology to cut region and a Kozak consensus and the GAL4 gene to induce homology directed repair (HDR) in embryos expressing Cas9 in germline (Figure 3B). Strains were established, and PCR showed that the replacement of the gene coding sequence with GAL4 was precise. Also, the transcript for *wdr37* could not be detected by RT-PCR in *trans*-heterozygous animals containing the allele over a molecularly defined deficiency, *Df(3R)Exel6179*,[22] that removes *wdr37* (Figure 3C). These data ensured that we generated a genetic null allele named $wdr37^{GAL4\Delta}$.

Upon crossing $wdr37^{GAL4\Delta}$ animals with UAS-GFP, we noted that the gene is widely and highly expressed throughout the body in larval stages and adult flies (Figure 4A), in agreement with high throughput expression profiling data.[23] As the symptoms in the probands were predominantly neurological, we further analyzed the expression pattern of *wdr37* in the central nervous system. We stained adult brains of $wdr37^{GAL4\Delta}$*; UAS-nuclear localization signal (nls)GFP* with the nuclear neuronal marker Elav (Embryonic Lethal Abnormal Vision) or the

Table 3. *De Novo WDR37* Variants

Variant Details	Proband 1	Proband 2	Proband 3	Proband 4	Proband 5
cDNA (NM_014023.3); gDNA (Chr10,GRCh37); Protein	c.374C>T; g.1126394C>T; p.Thr125Ile	c.386C>G; g.1126406C>G; p.Ser129Cys	c.356C>T; g.1126376C>T; p.Ser119Phe	c.386C>G; g.1126406C>G; p.Ser129Cys	c.389C>T; g.1126409C>T; p.Thr130Ile
CADD Phred score	32	27.7	29.5	27.7	25
MutationTaster probability[a]	1	1	1	1	1
SIFT[b]	score: 0.03, median: 3.57	score: 0.05, median: 3.57	score: 0.03, median: 3.57	score: 0.05, median: 3.57	score: 0, median: 3.97
PolyPhen	probably damaging	probably damaging	probably damaging	probably damaging	benign
PROVEAN	deleterious	deleterious	deleterious	deleterious	deleterious

Note that all variants are *de novo* and are not present in ExAc or gnomAD. Abbreviations: CADD, Combined Annotation Dependent Depletion; PolyPhen, Poly morphism Phenotyping; PROVEAN, Protein Variation Effect Analyzer.
[a]All variants are disease-causing according to MutationTaster
[b]All variants are deleterious as predicted by Sorting Intolerant From Tolerant (SIFT) software

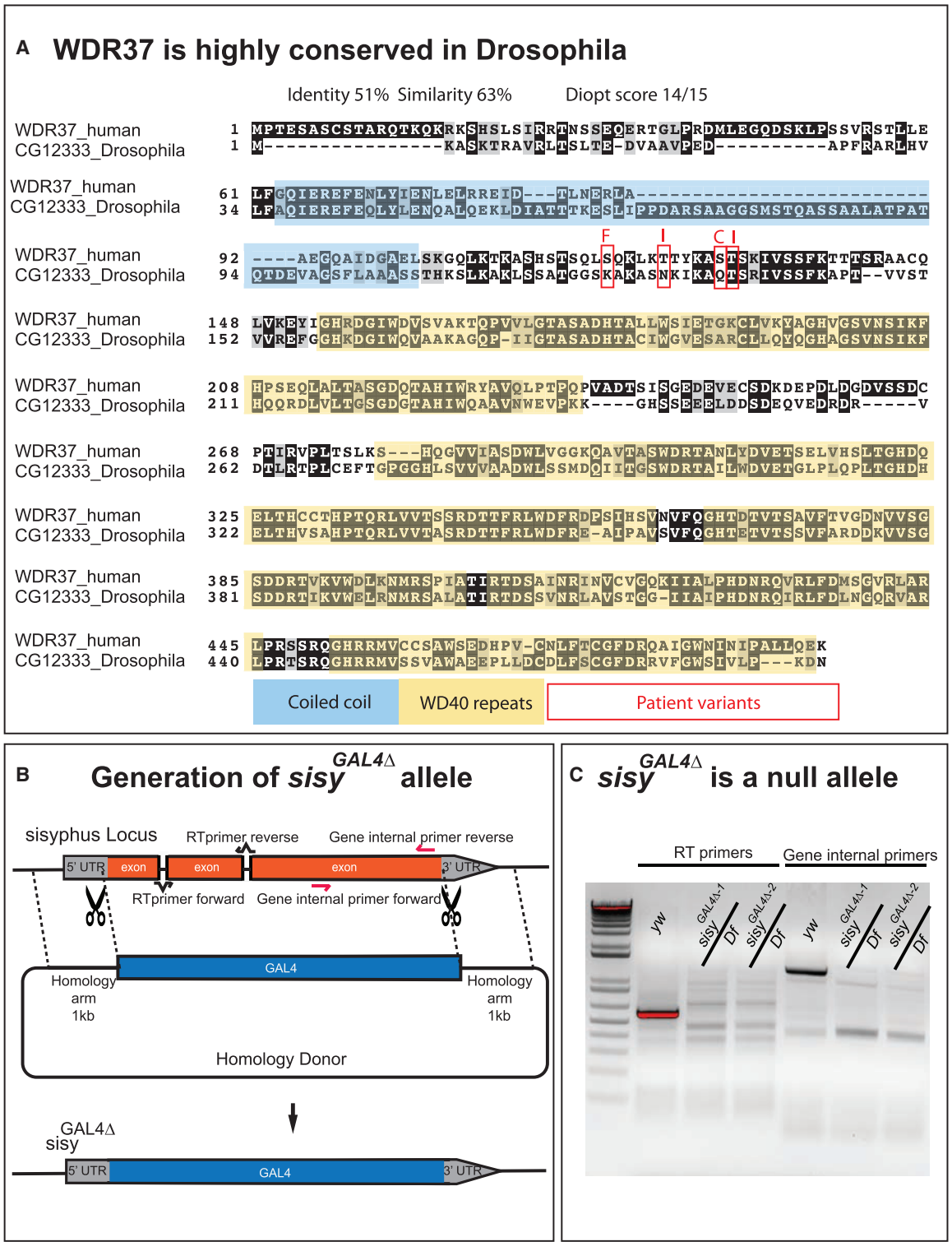

Figure 3. Conservation of *WDR37* and Generation of *wdr37*-Null Allele
(A) Alignment of *WDR37* with *wdr37*. Protein domains of WDR37 were identified through UniProt and SMART databases. The variants identified in the probands are marked with a red box and variant residue is indicated above the variant amino acid. WD40 repeats are shaded yellow and the coiled coil region is shaded blue.
(B) Generation of $wdr37^{GAL4\Delta}$ allele. Primer sites to verify the insertion are indicated on the construct.
(C) RT-PCR confirmation of *wdr37*-null alleles. RNA is isolated and reverse transcribed from two independent lines of $wdr37^{GAL4\Delta}$ / *Def(3R)6179* and *yw* flies as control. Correct amplicons are detected only in the *yw* animals.

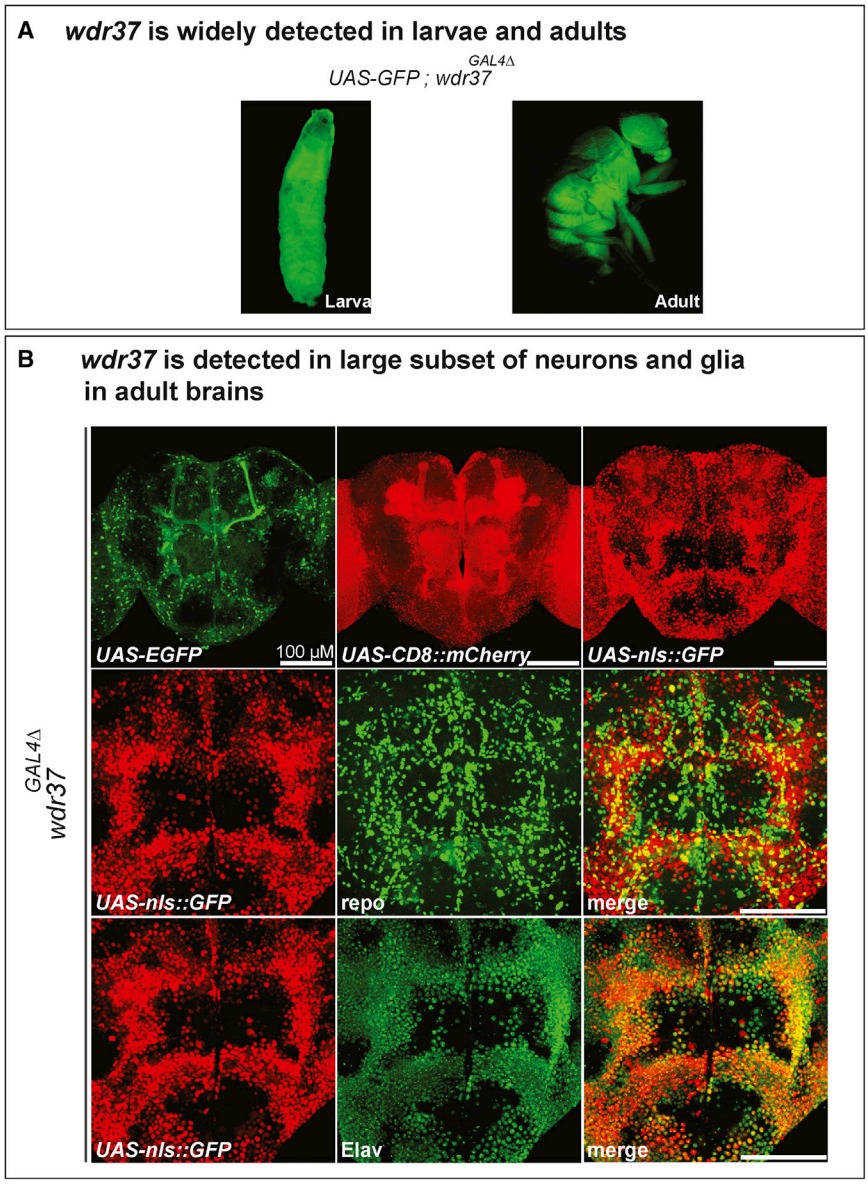

Figure 4. Expression of *wdr37* in Adults and Larvae

(A) Expression of *UAS-GFP* under the control of $wdr37^{GAL4\Delta}$ is monitored in larval and adult body.

(B) Expression domain of *wdr37* is monitored in adult brain by using the indicated transgenes. Co-staining with neuronal marker (ElaV) and glial marker (repo) indicate that the gene is expressed in large subsets of neurons and glia.

nuclear glial marker Repo (Reversed Polarity). As shown in Figure 4B, *wdr37* is expressed in most neurons and glia of the adult brains.

Null mutant animals ($wdr37^{GAL4\Delta}/wdr37^{GAL4\Delta}$ or $wdr37^{GAL4\Delta}/Df(3R)Exel6179$) were viable and fertile and did not display obvious morphological phenotypes. We therefore turned to behavioral assays. A key phenotype linked to epilepsy in humans is bang sensitivity in flies.[24,25] Bang sensitivity measures the time that the flies take to right themselves and move after a mechanical stress (such as a 30 s vortex in a tube). Wild-type (WT) flies right themselves instantaneously whereas bang-sensitive flies show stereotypical cycles of paralysis followed by uncoordinated limb movements for several seconds to a minute. This uncoordinated movement sequence resembles seizures and typically can be suppressed by several anti-convulsive drugs.[24,26,27] Comparison of $wdr37^{GAL4\Delta}/Df(3R)Exel6179$ animals to heterozygous animals ($wdr37^{GAL4\Delta}$ /+ or $Df(3R)Exel6179$ /+) showed that *wdr37*-null flies are severely bang sensitive and remain uncoordinated for ~10–30 s after mechanical stress (Figure 5A).

Next, we assessed the ability of flies to climb. When flies are tapped down to the bottom of a vial, they immediately start to climb up the side of the vial through negative geotaxis.[28] Control flies reach the top of the vial (6.5 cm) within a few seconds and typically stay just below the cotton plug of the vial; 13% of flies fall within 30 s of recording (Video S1). Interestingly, the majority of *wdr37* mutants reached the top of the vial quickly but 57% of the flies fall within a 30 s recording period. They seem not to be able to hold their grip during this action (Video S2) and repeat this cycle of climbing and falling. It is interesting to note that the mice that lack *Wdr37* exhibit a "low grip strength phenotype."[13] Given that *wdr37* is broadly expressed in CNS and muscles, it is not obvious whether the defect is neurological or muscular in nature.

The third behavioral phenotype we evaluated was *Drosophila* courtship, a form of stereotyped social behavior that is composed of a number of sequential steps required for the initiation of copulation, including tapping, wing vibration, and licking the female abdomen.[29] Initial comparisons between $wdr37^{GAL4\Delta}$ /*Df(3R)Exel6179* and wild-type CantonS flies revealed a positioning defect during copulation. Normally, male *Drosophila* typically cling to the backside of the females when mating, maintaining their position by gripping the female's abdomen with their legs (Figure 5B and Video S3). Null animals were incapable of maintaining their grip on the female during copulation, with 71% of the flies failing to maintain typical copulatory posture or visibly flailing four or more limbs during the mating process (Figure 5B and Video S4).

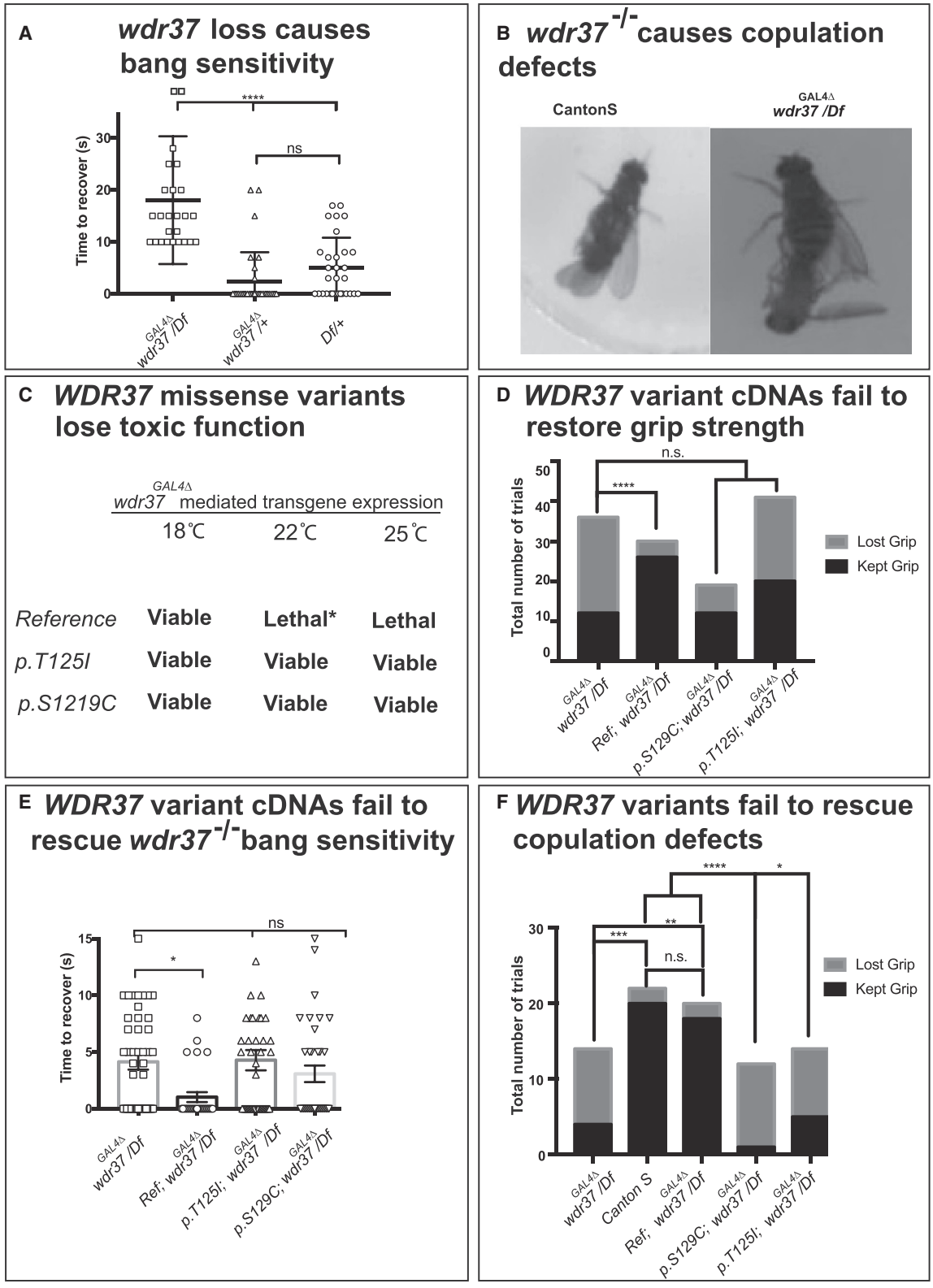

Figure 5. Adult Phenotypes of *wdr37*-Null Mutants

(A) *wdr37* (*wdr37*$^{GAL4\Delta}$ */Df*)-null flies exhibit bang sensitivity. *Df* corresponds to *Df(3R)Exel6179*.

(B) Males of the indicated genotype in the presence of wild-type (CantonS) females are visualized for 30 min. Wild-type males (on the left) can maintain their grip of female abdomen during copulation whereas the *wdr37*$^{GAL4\Delta}$*/ Df(3R)6179* males often lose their grip and are unable to maintain normal copulatory posture.

(C) Overexpression of the *UAS-WDR37* human reference cDNA under the control of *wdr37*$^{GAL4\Delta}$ is toxic at 25°C and 22°C (with <5% that survive and are referred to as "escapers"); this toxicity is suppressed at 18°C. The *UAS-WDR37* lines with the human variant cDNAs lose this toxicity.

(legend continued on next page)

To rescue the bang sensitivity, grip weakness, and copulation defect, we tested whether the GAL4 that replaced the *wdr37* coding sequence could drive the UAS-human *WDR37* cDNA and rescue these phenotypes.[16,30] We generated transgenic flies with *UAS-WDR37* full-length reference cDNAs and two of the variant cDNAs, p.Thr125Ile and p.Ser129Cys. The cDNA constructs were cloned in identical vectors and inserted in the same genomic landing site, minimizing genetic background variation with different experimental conditions. By comparing their rescue ability, we can evaluate whether the variants impair protein function even when the amino acids are not evolutionarily conserved. With this system, we can also alter the expression level of human cDNAs by raising the flies at different temperatures; at 25°C the expression of UAS-cDNA is often significantly higher and can be sometimes toxic, when compared to 18°C.[31] We found that at 25°C the expression of the UAS reference human cDNA driven by $wdr37^{GAL4\Delta}$ induced pupal lethality, while the *WDR37* cDNAs carrying the proband variants (p.Thr125Ile and p.Ser129Cys) were viable and fertile when raised at 25°C (Figure 5C). These data indicate that the variants are less toxic than the reference cDNA and are likely associated with a loss of function, at least when tested in flies.

To determine whether the human reference *WDR37* cDNA and the variants can rescue the *wdr37*-null mutant bang sensitivity, decreased grip strength, and courtship behavior phenotypes, the flies were raised at 18°C. The human reference *WDR37* expressed at 18°C under the control of $wdr37^{GAL4\Delta}$ nearly fully rescued all three phenotypes (Figures 5D–5F). Note that at this temperature the bang sensitivity is milder than at 25°C. However, neither of the two tested human cDNA variants rescue the phenotypes associated with the loss of *wdr37*, again indicating that the two variants cause a loss of function.

In summary, we identified five individuals with overlapping neurological phenotypes that have *de novo* missense variants that map to a small region of *WDR37*. Clinically, all of them had eye anomalies (mostly bilateral colobomas), dysmorphic features, seizures, feeding difficulties, developmental delay, intellectual disability, and no verbal development; most of the probands had congenital cardiac defects and hypotonia. Brain imaging studies demonstrated several consistent abnormalities including mildly simplified gyral pattern with relatively shallow sulci, small and dysplastic hippocampi, mild to moderate reduced volume of white matter, mild ventriculomegaly, diffusely thin corpus callosum, mildly thin brainstem with small pons, and moderately diffuse cerebellar and vermis hypoplasia with a striking foliar dysplasia. Despite the similarities, there are features that are not present in all probands, or specific to a single proband. For example, proband 4 exhibited spastic quadriplegia, while the others manifested with hypotonia; only proband 1 had significant neuroregression. Probands 1 and 2 both presented with respiratory issues, but we cannot be certain that the *WDR37* variants are responsible for this phenotype. While all probands had pathogenic variants in *WDR37*, it is possible that some of the variabilities in the clinical presentation can be secondary to other unknown genetic background or other environmental factors unique to each proband. The identification of additional individuals with variants in *WDR37*, together with a more detailed characterization of the natural progression of disease, will help define *WDR37*-related disorders.

The human reference WDR37 protein can functionally replace the fly ortholog, *wdr37*, showing a molecular conservation of the function of the proteins. Moreover, there are some phenotypic parallels including epilepsy in probands and bang sensitivity in flies. All probands in this cohort carry *de novo*, monoallelic missense variants, indicating dominance. Alleles can cause dominant phenotypes through haploinsufficiency, gain-of-function, or dominant-negative mechanisms. Haploinsufficiency was not observed in flies and mice. Moreover, the probands with CNVs of *WDR37* and adjacent genes share limited phenotypic similarity with our cohort and three individuals were documented in the gnomAD control populations with heterozygous early frameshift alleles. These data suggest that the *WDR37* variants identified in our probands are unlikely to be simple LoF alleles. A gain-of-function mechanism in flies, however, is unlikely given that the expression of the human variants in mutant flies do not exacerbate the phenotype and act as loss-of-function alleles. Further studies will be required to determine whether the variants found in our probands act as dominant-negative mutations. Follow-up studies using vertebrates, cell models, and human tissue will lead to a better insight into the precise function of this gene and a detailed understanding of disease mechanism.

Accession Numbers

The variants in this study have been submitted to ClinVar, with the following accession numbers: NM_014023.3:c.374C>T, SCV000920632; NM_014023.3:c.386C>G, SCV000920633; NM_014023.3:c.356C>T, SCV000920634; NM_014023.3:c.389C>T, SCV000920635.

(D) *wdr37*-null flies ($wdr37^{GAL4\Delta}$/*Df*) show negative geotaxis but fail to hang on the surface of the vial for 30 s; this phenotype is rescued by the full-length *UAS WDR37* reference cDNA (*Ref*) but not rescued by neither of the variant cDNAs (*p.T125I* or *p.S129C*).
(E) The loss of *wdr37* leads to increased bang sensitivity, which is rescued by the human reference cDNA (*Ref*), but not the variants *p.T125I* or *p.S129C*. Note that the duration of bang sensitivity response is shorter at experimental temperature.
(F) The reference human cDNA (*Ref*) can rescue the copulation defect whereas *p.S129C* and *p.T125I* variant cDNAs fail to rescue copulation defect. *Ref* indicates line with *UAS-WDR37* full-length cDNA human reference, *p.T125I* indicates variant *UAS-WDR37* with the p.T125I variant, and *p.S129C* indicates variant *UAS-WDR37* with the p.S129C variant. *$p \leq 0.05$, **$p \leq 0.01$, ***$p \leq 0.001$, and ****$p \leq 0.0001$. ns indicates not significant.

Supplemental Data

Supplemental Data can be found online at https://doi.org/10.1016/j.ajhg.2019.06.014.

Acknowledgments

We thank the probands and their families for participating in this study. We thank Dr. Jessica Tenney and Dr. Balram Gangaram (UCSF) for their inputs on proband 3, and Dr. Jill Madden (The Manton Center, Boston Children's Hospital) for facilitating data collection for proband 5. This paper is supported in part by The Common Fund of the NIH, Office of the Director; NIH NHGRI Intramural Research Grant; NIH grants U54NS093793 to H.J.B., M.F.W., and S.Y.; R24OD022005 and R01GM067858 to H.J.B.; 1F32 NS110174-01 Fellowship award to J.C.A.; Simons Foundation Autism Research Initiative (Award#368479) to M.F.W. and S.Y.; and SFARI and the JPB Foundation (W.K.C). We are thankful for the technical assistance provided by Y. Huang (NIH UDP Translational Laboratory) for Sanger sequencing and Ellen Macnamara for facilitating confirmation of mutation in proband 1. We thank the Bloomington Drosophila Stock Center, Drosophila Genomics and Genetic Resources, and FlyORF for numerous stocks and the Developmental Studies Hybridoma Bank for antibodies. This study made use of data generated by the DECIPHER community; a full list of centers that contributed to the generation of the data is available at https://decipher.sanger.ac.uk and via email at decipher@sanger.ac.uk; funding for the project was provided by the Wellcome Trust. H.J.B. is an investigator of the Howard Hughes Medical Institute. The content is solely the responsibility of the authors and does not necessarily represent the official views of the National Institutes of Health.

Declaration of Interests

The authors declare no competing interests.

Received: November 18, 2018
Accepted: June 14, 2019
Published: July 18, 2019

Web Resources

1000 Genomes, http://www.internationalgenome.org/
CADD, https://cadd.gs.washington.edu/
ClinVar, https://www.ncbi.nlm.nih.gov/clinvar/
dbSNP, https://www.ncbi.nlm.nih.gov/projects/SNP/
DECIPHER, https://decipher.sanger.ac.uk/
DIOPT, https://www.flyrnai.org/cgi-bin/DRSC_orthologs.pl
ExAC, http://exac.broadinstitute.org/
Genematcher, https://genematcher.org/
Geno2MP, https://geno2mp.gs.washington.edu/Geno2MP/#/
gnomAD Browser, https://gnomad.broadinstitute.org
HUGO Gene Nomenclature Committee, https://www.genenames.org/
IMPC, https://www.mousephenotype.org/data/genes/MGI:1920393
MARRVEL, http://marrvel.org
OMIM, https://omim.org/
PolyPhen-2, http://genetics.bwh.harvard.edu/pph2/
PROVEAN, http://provean.jcvi.org/
SIFT, http://sift.jcvi.org

References

1. Stirnimann, C.U., Petsalaki, E., Russell, R.B., and Müller, C.W. (2010). WD40 proteins propel cellular networks. Trends Biochem. Sci. *35*, 565–574.
2. Zou, X.D., Hu, X.J., Ma, J., Li, T., Ye, Z.Q., and Wu, Y.D. (2016). Genome-wide Analysis of WD40 Protein Family in Human. Sci. Rep. *6*, 39262.
3. Brownstein, C.A., Holm, I.A., Ramoni, R., Goldstein, D.B.; and Members of the Undiagnosed Diseases Network (2015). Data sharing in the undiagnosed diseases network. Hum. Mutat. *36*, 985–988.
4. Gahl, W.A., Markello, T.C., Toro, C., Fajardo, K.F., Sincan, M., Gill, F., Carlson-Donohoe, H., Gropman, A., Pierson, T.M., Golas, G., et al. (2012). The National Institutes of Health Undiagnosed Diseases Program: insights into rare diseases. Genet. Med. *14*, 51–59.
5. Gahl, W.A., Mulvihill, J.J., Toro, C., Markello, T.C., Wise, A.L., Ramoni, R.B., Adams, D.R., Tifft, C.J.; and UDN (2016). The NIH Undiagnosed Diseases Program and Network: Applications to modern medicine. Mol. Genet. Metab. *117*, 393–400.
6. Sobreira, N., Schiettecatte, F., Valle, D., and Hamosh, A. (2015). GeneMatcher: a matching tool for connecting investigators with an interest in the same gene. Hum. Mutat. *36*, 928–930.
7. Chong, J.X., Yu, J.H., Lorentzen, P., Park, K.M., Jamal, S.M., Tabor, H.K., Rauch, A., Saenz, M.S., Boltshauser, E., Patterson, K.E., et al. (2016). Gene discovery for Mendelian conditions via social networking: de novo variants in KDM1A cause developmental delay and distinctive facial features. Genet. Med. *18*, 788–795.
8. Richards, S., Aziz, N., Bale, S., Bick, D., Das, S., Gastier-Foster, J., Grody, W.W., Hegde, M., Lyon, E., Spector, E., et al.; ACMG Laboratory Quality Assurance Committee (2015). Standards and guidelines for the interpretation of sequence variants: a joint consensus recommendation of the American College of Medical Genetics and Genomics and the Association for Molecular Pathology. Genet. Med. *17*, 405–424.
9. Wang, J., Al-Ouran, R., Hu, Y., Kim, S.Y., Wan, Y.W., Wangler, M.F., Yamamoto, S., Chao, H.T., Comjean, A., Mohr, S.E., et al.; UDN (2017). MARRVEL: Integration of Human and Model Organism Genetic Resources to Facilitate Functional Annotation of the Human Genome. Am. J. Hum. Genet. *100*, 843–853.
10. Lek, M., Karczewski, K.J., Minikel, E.V., Samocha, K.E., Banks, E., Fennell, T., O'Donnell-Luria, A.H., Ware, J.S., Hill, A.J., Cummings, B.B., et al.; Exome Aggregation Consortium (2016). Analysis of protein-coding genetic variation in 60,706 humans. Nature *536*, 285–291.
11. Firth, H.V., Richards, S.M., Bevan, A.P., Clayton, S., Corpas, M., Rajan, D., Van Vooren, S., Moreau, Y., Pettett, R.M., and Carter, N.P. (2009). DECIPHER: Database of Chromosomal Imbalance and Phenotype in Humans Using Ensembl Resources. Am. J. Hum. Genet. *84*, 524–533.
12. Auton, A., Brooks, L.D., Durbin, R.M., Garrison, E.P., Kang, H.M., Korbel, J.O., Marchini, J.L., McCarthy, S., McVean, G.A., Abecasis, G.R.; and 1000 Genomes Project Consortium (2015). A global reference for human genetic variation. Nature *526*, 68–74.
13. Dickinson, M.E., Flenniken, A.M., Ji, X., Teboul, L., Wong, M.D., White, J.K., Meehan, T.F., Weninger, W.J., Westerberg, H., Adissu, H., et al.; International Mouse Phenotyping Consortium; Jackson Laboratory; Infrastructure Nationale

PHENOMIN, Institut Clinique de la Souris (ICS); Charles River Laboratories; MRC Harwell; Toronto Centre for Phenogenomics; Wellcome Trust Sanger Institute; RIKEN BioResource Center (2016). High-throughput discovery of novel developmental phenotypes. Nature *537*, 508–514.
14. Chow, C.Y., and Reiter, L.T. (2017). Etiology of Human Genetic Disease on the Fly. Trends Genet. *33*, 391–398.
15. Şentürk, M., and Bellen, H.J. (2018). Genetic strategies to tackle neurological diseases in fruit flies. Curr. Opin. Neurobiol. *50*, 24–32.
16. Oriel, C., and Lasko, P. (2018). Recent Developments in Using *Drosophila* as a Model for Human Genetic Disease. Int. J. Mol. Sci. *19*, 19.
17. Hu, Y., Flockhart, I., Vinayagam, A., Bergwitz, C., Berger, B., Perrimon, N., and Mohr, S.E. (2011). An integrative approach to ortholog prediction for disease-focused and other functional studies. BMC Bioinformatics *12*, 357.
18. Haurwitz, R.E., Jinek, M., Wiedenheft, B., Zhou, K., and Doudna, J.A. (2010). Sequence- and structure-specific RNA processing by a CRISPR endonuclease. Science *329*, 1355–1358.
19. Gratz, S.J., Cummings, A.M., Nguyen, J.N., Hamm, D.C., Donohue, L.K., Harrison, M.M., Wildonger, J., and O'Connor-Giles, K.M. (2013). Genome engineering of Drosophila with the CRISPR RNA-guided Cas9 nuclease. Genetics *194*, 1029–1035.
20. Lee, P.T., Zirin, J., Kanca, O., Lin, W.W., Schulze, K.L., Li-Kroeger, D., Tao, R., Devereaux, C., Hu, Y., Chung, V., et al. (2018). A gene-specific *T2A-GAL4* library for *Drosophila*. eLife *7*, 7.
21. Brand, A.H., and Perrimon, N. (1993). Targeted gene expression as a means of altering cell fates and generating dominant phenotypes. Development *118*, 401–415.
22. Ryder, E., Blows, F., Ashburner, M., Bautista-Llacer, R., Coulson, D., Drummond, J., Webster, J., Gubb, D., Gunton, N., Johnson, G., et al. (2004). The DrosDel collection: a set of P-element insertions for generating custom chromosomal aberrations in Drosophila melanogaster. Genetics *167*, 797–813.
23. Leader, D.P., Krause, S.A., Pandit, A., Davies, S.A., and Dow, J.A.T. (2018). FlyAtlas 2: a new version of the Drosophila melanogaster expression atlas with RNA-Seq, miRNA-Seq and sex-specific data. Nucleic Acids Res. *46* (D1), D809–D815.
24. Kuebler, D., and Tanouye, M.A. (2000). Modifications of seizure susceptibility in Drosophila. J. Neurophysiol. *83*, 998–1009.
25. Parker, L., Howlett, I.C., Rusan, Z.M., and Tanouye, M.A. (2011). Seizure and epilepsy: studies of seizure disorders in Drosophila. Int. Rev. Neurobiol. *99*, 1–21.
26. Kuebler, D., and Tanouye, M. (2002). Anticonvulsant valproate reduces seizure-susceptibility in mutant Drosophila. Brain Res. *958*, 36–42.
27. Song, J., and Tanouye, M.A. (2008). From bench to drug: human seizure modeling using Drosophila. Prog. Neurobiol. *84*, 182–191.
28. Gargano, J.W., Martin, I., Bhandari, P., and Grotewiel, M.S. (2005). Rapid iterative negative geotaxis (RING): a new method for assessing age-related locomotor decline in Drosophila. Exp. Gerontol. *40*, 386–395.
29. Villella, A., and Hall, J.C. (2008). Neurogenetics of courtship and mating in Drosophila. Adv. Genet. *62*, 67–184.
30. Salazar, J.L., and Yamamoto, S. (2018). Integration of Drosophila and Human Genetics to Understand Notch Signaling Related Diseases. Adv. Exp. Med. Biol. *1066*, 141–185.
31. Nagarkar-Jaiswal, S., Lee, P.T., Campbell, M.E., Chen, K., Anguiano-Zarate, S., Gutierrez, M.C., Busby, T., Lin, W.W., He, Y., Schulze, K.L., et al. (2015). A library of MiMICs allows tagging of genes and reversible, spatial and temporal knockdown of proteins in Drosophila. eLife *4*, 4.
32. Sanchez, C.E., Richards, J.E., and Almli, C.R. (2012). Neurodevelopmental MRI brain templates for children from 2 weeks to 4 years of age. Dev. Psychobiol. *54*, 77–91.